Dynamics of radiocaesium within forests in Fukushima-results and analysis of a model inter-comparison

Shoji Hashimoto, Taku Tanaka, Masabumi Komatsu, Marc Andre Gonze, Wataru Sakashita, Hiroshi Kurikami, Kazuya Nishina, Masakazu Ota, Shinta Ohashi, Philippe Calmon, et al.

Journal of Environmental Radioactivity 238-239 (2021) 106721

Contents lists available at ScienceDirect

Journal of Environmental Radioactivity

journal homepage: www.elsevier.com/locate/jenvrad

Dynamics of radiocaesium within forests in Fukushima—results and analysis of a model inter-comparison

Shoji Hashimoto [a,b,*], Taku Tanaka [c,**], Masabumi Komatsu [d,e], Marc-André Gonze [f], Wataru Sakashita [a,e], Hiroshi Kurikami [g], Kazuya Nishina [h], Masakazu Ota [i], Shinta Ohashi [j,e], Philippe Calmon [f], Frederic Coppin [f], Naohiro Imamura [a], Seiji Hayashi [k], Keizo Hirai [a], Pierre Hurtevent [f], Jun Koarashi [i], Takuya Manaka [a], Satoru Miura [e], Yoshiki Shinomiya [e], George Shaw [l], Yves Thiry [m]

[a] Department of Forest Soils, Forestry and Forest Products Research Institute, Tsukuba, Ibaraki, 305-8687, Japan
[b] Graduate School of Agricultural and Life Sciences, The University of Tokyo, Bunkyo-ku, Tokyo, 113-8657, Japan
[c] EDF R&D, LNHE, 6 Quai Watier, 78400, Chatou, France
[d] Department of Mushroom Science and Forest Microbiology, Forestry and Forest Products Research Institute, Tsukuba, Ibaraki, 305-8687, Japan
[e] Center for Forest Restoration and Radioecology, Forestry and Forest Products Research Institute, Tsukuba, Ibaraki, 305-8687, Japan
[f] Institute of Radiation Protection and Nuclear Safety, PSE-ENV, CE Cadarache-Bat 153, BP3, 13115, St-Paul-lez-Durance cedex, France
[g] Fukushima Environmental Research Group, Japan Atomic Energy Agency, 10-2 Fukasaku, Miharu-machi, Tamura-gun, Fukushima, 963-7700, Japan
[h] Earth System Division, National Institute for Environmental Studies, Tsukuba, 305-8506, Japan
[i] Research Group for Environmental Science, Japan Atomic Energy Agency, 2-4 Shirakata, Tokai, Ibaraki, 319-1195, Japan
[j] Department of Wood Properties and Processing, Forestry and Forest Products Research Institute, Tsukuba, Ibaraki, 305-8687, Japan
[k] Fukushima Regional Collaborative Research Center, National Institute for Environmental Studies,10-2 Fukasaku, Miharu, Fukushima, 963-7700, Japan
[l] School of Biosciences, University of Nottingham, Sutton Bonington, LE12 5RD, UK
[m] Andra, Research and Development Division, 1-7 Rue Jean-Monnet, 92298, Châtenay-Malabry cedex, France

ARTICLE INFO

Keywords:
Radiocesium dynamics and cycling
^{137}Cs migration and transfer
Forest ecosystem
Fukushima accident
Model simulation and prediction
Tree and soil

ABSTRACT

Forests cover approximately 70% of the area contaminated by the Fukushima Daiichi Nuclear Power Plant accident in 2011. Following this severe contamination event, radiocaesium (^{137}Cs) is anticipated to circulate within these forest ecosystems for several decades. Since the accident, a number of models have been constructed to evaluate the past and future dynamics of ^{137}Cs in these forests. To explore the performance and uncertainties of these models we conducted a model inter-comparison exercise using Fukushima data. The main scenario addressed an evergreen needleleaf forest (cedar/cypress), which is the most common and commercially important forest type in Japan. We also tested the models with two forest management scenarios (decontamination by removal of soil surface litter and forest regeneration) and, furthermore, a deciduous broadleaf forest (konara oak) scenario as a preliminary modelling study of this type of forest. After appropriate calibration, the models reproduced the observed data reliably and the ranges of calculated trajectories were narrow in the early phase after the fallout. Successful model performances in the early phase were probably attributable to the availability of comprehensive data characterizing radiocaesium partitioning in the early phase. However, the envelope of the calculated model end points enlarged in long-term simulations over 50 years after the fallout. It is essential to continue repetitive verification/validation processes using decadal data for various forest types to improve the models and to update the forecasting capacity of the models.

1. Introduction

In the spring of 2011, radioactive isotopes of caesium (^{134}Cs and ^{137}Cs) were released due to the Fukushima Daiichi Nuclear Power Plant (FDNPP) accident and deposited on both terrestrial and marine environments. Approximately 70% of the Japanese land area affected by the

* Corresponding author. Department of Forest Soils, Forestry and Forest Products Research Institute, Tsukuba, Ibaraki, 305-8687, Japan.
** Corresponding author. EDF R&D, LNHE, 6 Quai Watier, 78400, Chatou, France.
E-mail addresses: shojih@ffpri.affrc.go.jp (S. Hashimoto), taku.tanaka@edf.fr (T. Tanaka).

https://doi.org/10.1016/j.jenvrad.2021.106721
Received 2 June 2021; Received in revised form 9 August 2021; Accepted 13 August 2021
Available online 8 September 2021

radioactive fallout is forested (Gonze et al., 2014; Hashimoto et al., 2012). Due to the long half-life of ^{137}Cs (30.2 years) and its capacity to integrate into natural biogeochemical cycles of elements (Goor and Thiry, 2004), the spatio-temporal dynamics of radiocaesium within forests are of great concern in contaminated forests within the Fukushima region. Therefore, understanding and reliable prediction of the radiocaesium dynamics within forest ecosystems are essential and, for these purposes, robust models are needed.

The earliest investigations and models focusing on radiocaesium behavior in forest ecosystems have revealed the importance of recycling of this radionuclide between soil and perennial vegetation, leading to the potential persistence of radiocaesium in standing biomass and forest topsoil (Croom and Ragsdale, 1980; Olson, 1965). Post-Chernobyl and -Fukushima radioecological research has confirmed these general features as well as the potential for long-lasting human radiation exposure due to contamination of different forest products (e.g. timber, berries and mushrooms) with radiocaesium (IAEA, 2015; 2006). Forest functioning involves continuous cycling of elements such as potassium, of which caesium is an analogue. Depending mostly on edaphic conditions that largely control radiocaesium bioavailability in soils, it can take decades for radiocaesium fluxes to reach equilibrium between soil and trees (Shaw, 2007; Shcheglov et al., 2014; Thiry et al., 2018). Due to the complexity and longevity of forest ecosystems, modelling provides a logical approach for understanding and quantifying the long-term partitioning of radioactive fallout in contaminated forest areas. Mathematical models provide valuable tools for interpreting and generalizing the numerous data collected at specific study sites and at different times after the fallout (Diener et al., 2017; Gonze et al., 2021). In view of the complex transfers controlling radiocaesium cycling in forests, we also need models as research tools to represent combinations of ecosystem processes to achieve the optimal representation of the whole cycle. Models can provide additional support to inform and refine the necessary long-term studies in field monitoring. Finally, well-validated models may be useful predictive tools for forest managers and decision makers in attempts to provide forecasts of the effects of different remediation or management strategies. The FDNPP accident has stimulated debate on the effectiveness of countermeasures by forest management actions such as thinning of trees in the affected areas. In his review on post-Chernobyl research on behavior of radiocaesium in forests, Riesen (2002) suggested that radioecological forest models should be considered as research rather than assessment tools. Because forest radioecological models are still constrained by data and understanding of processes, they must be constantly upgraded based on newly obtained data and research findings (Fesenko et al., 1999; Riesen, 2002); recommendations provided by inter-comparison of different models can also help in this process (Avila et al., 2001; Shaw et al., 2003).

After the FDNPP accident, several modelling studies have been conducted for forests (Calmon et al., 2015; Hashimoto et al., 2013, 2020a; Kurikami et al., 2019; Nishina and Hayashi, 2015; Ota et al., 2016; Thiry et al., 2020). These studies focused on Fukushima data; however, calibration and validation were conducted using different datasets between the studies. Hence, variations between individual model predictions remain difficult to explain and the general reliability of these actively developing models is hard to assess. Similar difficulties were encountered in the IAEA's BIOMASS study (IAEA, 2002). This included a Forest Working Group which brought together experimental radioecologists with modelers to try to improve predictions of radiocaesium in forests, post-Chernobyl. As a group, the models could predict the broad spread of radiocaesium activity concentrations in diverse forest components over a limited time span of 12 years. However, there was considerable conceptual uncertainty between models which reflected the different approaches taken by individual modelers when using field data to make subsequent forecasts.

The aim of the study in this paper is to explore the comparative performance and uncertainties (specifically, inter-model variability) of state-of-the-art models of radiocesium circulation in forests, developed and/or updated after the Fukushima accident. We designed an evergreen needleleaf (Japanese cedar/hinoki cypress) forest scenario and tested six models. The modelers were allowed to reconfigure the structure of their models and parameterize them if necessary. We evaluated the models' performance before and after calibration and examined the variation of model trajectories using the range or 'envelope' of model outputs such as activity concentrations and inventories for wood. To further characterize the coherence between model predictions, the model outputs were extended to 50 years after the initial fallout. Moreover, two management scenarios (soil surface removal and tree cutting and replanting) were included in the study, as well as an ancillary scenario examining a deciduous (konara oak) forest to further explore and test the wider applicability of the models, which were originally developed for evergreen coniferous forests.

2. Materials and methods

2.1. Scenario description

2.1.1. Main test scenario – evergreen needleleaf forest (generic cedar and cypress: scenario A1)

This scenario (denoted as scenario A1) is representative of a typical coniferous plantation of Japanese cedar (*Cryptomeria japonica*) and hinoki cypress (*Chamaecyparis obtusa*) trees contaminated by atmospheric fallout from the FDNPP in March 2011. It relies on a comprehensive dataset of ^{137}Cs activities measured in aerial tree organs and soil layers over the period March 2011–March 2017, as well as on ^{137}Cs activity transferred to the forest floor by tree depuration mechanisms. This dataset was set up by Gonze et al. (2021) based on compilation, processing and averaging of site-specific field data extracted from the post-Fukushima literature. The review encompassed 37 forest sites mostly located in Fukushima Prefecture and Kanto region with a majority of mature cedar forests planted on andosols with a mean age of 45 years. To reduce variability among sites, all radiological measurements were interpolated onto the same spatio-temporal frame (i.e. time frequency, vertical discretization of soil) and normalized by the local deposit that typically varied from 10 kBq m^{-2} to 1000 kBq m^{-2} (decay corrected to March 15, 2011). The local deposits based on the field survey were used when reported. In other cases, the estimated local deposits based on the 4th airborne survey were used (Gonze et al., 2021). Please note that as a result of the normalization, the inventories and activity concentrations are unitless and m^2 kg^{-1} d.m. (dry mass), respectively. Such treatments reinforced the consistency between sites, although a poorly understood residual variability persisted that probably resulted from: (i) differences in the interception fraction, forest stand or climate characteristics, (ii) measurement errors, and (iii) uncertainties in the estimate of the initial deposit. As this residual noise was moderate with respect to the mean trend, the authors (Gonze et al., 2021) attempted to derive a generic evolution of ^{137}Cs over the 6-yr period by log-averaging observations over sites and quantifying the residual dispersion (geometric mean (GM) $\pm$ geometric standard deviation (GSD)). These mean dynamics were then analyzed with the help of simple mass balance equations. It was demonstrated that between 70% and 85% of the total radiocaesium deposit was probably intercepted by the canopies, this result being of particular interest in the present modelling study. More details are described elsewhere (Gonze et al., 2021).

2.1.2. Two management scenarios (scenarios B1 and B2)

We prepared two forest management scenarios to explore the model performance against management actions for remediation, notably the effectiveness of these actions in reducing tree contamination. The first management scenario is the removal of the soil surface organic layer (denoted as scenario B1), which was widely applied in Japan to reduce the exposure to ambient radiation near households and public buildings. Based on this management procedure, we assumed that 95% of the soil

surface was removed in September 2011, six months after the fallout.

The second management scenario is clear cutting and replanting of forests (denoted as scenario B2). In this management scenario, 100% of aboveground biomass was removed in March 2012 and exported from the forest site, and new cedar seedlings were planted. This radical option was often discussed after the FDNPP accident as a potential countermeasure to lower radiation dose in residential areas, and also to reduce the possible increase in activity concentration in wood in the future, although the effectiveness of this countermeasure is not known because it has never been widely applied in the real world.

It is important to note that the management scenarios were tested to examine the similarities/differences in model performance when applied to different possible forest management scenarios, not to suggest the best management practice and its timing (e.g. intensity, timing etc.) in this model inter-comparison.

2.1.3. Ancillary scenario – deciduous broadleaf forest (konara oak: scenario C1)

The models were applied to a deciduous broad leaf forest, specifically a konara oak (*Quercus serrata*) forest; this scenario was designed to provide a preliminary exploration of the applicability of the models since none of the models had been specifically developed using data from such forests. This scenario for deciduous broadleaf forests was based on a long-term monitoring site operated by the Forestry and Forest Products Research Institute, Japan. The site is located in Kawauchi Village in Fukushima Prefecture (37°17′22″N, 140°47′30″E), about 27 km southwest from the FDNPP. The dominant tree species at this site is konara oak, but other tree species including Japanese chestnut (*Castanea crenata*) and mizunara oak (*Quercus crispula*) are also present. The stand age of konara oak was 26 years in 2011. The estimated initial deposition of ^{137}Cs (decay corrected to March 11, 2011) was 504 kBq m^{-2}. The observation of radioactivity started in 2012; biomass, activity concentrations and inventories for leaf, branches, bark, wood, soil organic layers, and mineral soils have been measured in August every subsequent year (2012–2018). The data were decay-corrected to the appropriate sampling dates, and the values normalized by the total inventory in 2012 were shown in this study. Details of the site conditions are reported by Imamura et al. (2017); the plot name in this publication is"KU1-Q". The original data for this site can be found in the report by the Forestry Agency (https://www.rinya.maff.go.jp/j/kaihatu/jyosen/H30_jittaihaaku.html).

2.2. Participating models

Six models joined this exercise and are listed in Table 1; details of the models are described briefly in Supplementary Information and the literature references in Table 1. The characteristics of the participating models are described in Table 2 focusing on the model structures, processes, parameters and numerical approaches. The processes described in each model are diverse. Some models distinguish the forest functional compartments (e.g. foliage, branches, wood and bark), while others describe the lumped compartment (e.g. tree external surface). In general, the approaches taken by the participating models represent the transfers of radiocaesium between each of these compartments as constant (or time-dependent) kinetic rates. The varying level of complexity can be demonstrated by the types of processes and the number of parameters involved in each model: some models incorporate hydrological processes and tree biomass dynamics with a large number of parameters while others just describe the radionuclide dynamics with a limited number of parameters.

Table 1
The participating models and their key references.

Model name	Modeller (s)	Key references
CMFW	H. Kurikami	Kurikami et al. (2019)
FoRothCs	K. Nishina and S. Hayashi	Nishina et al. (2018); Nishina and Hayashi (2015)
RIFE1	S. Hashimoto and G. Shaw	Hashimoto et al. (2013) and (2020a)
SOLVEG-II	M. Ota and J. Koarashi	Ota et al. (2016)
TREE4	M-A. Gonze, P. Calmon, P. Hurtevent, P. Coppin	Calmon et al. (2015); Gonze et al. in prep.
TRIPS	Y. Thiry and T. Tanaka	Thiry et al. (2020), (2018)

In addition, model calibration processes vary between the participating models. Ratio *B/A* in Table 2 expresses the ratio of the number of parameters adjusted for calibration (*B*) to the total number of parameters (*A*). Modelling approaches with low *B/A* ratios (e.g. FoRothCs: 0.09, TRIPS2.0: 0.11, TREE4: 0.2, and SOLVEG-II: 0.22) can be regarded as the "forward" approach, which means that many of the parameter values were derived based on literature survey in advance of using measured endpoints for model calibration. Those with high ratios (e.g., CMFW: 1.0 and RIFE1: 0.64) can be regarded as the "inverse" approach, which means that many or all of the parameters were back-calculated using measured endpoints.

2.3. Protocols

In this exercise, we did not conduct a classical blind validation because most participating models were developed and parameterized after the FDNPP accident based, in part, on data presented in the scenarios of this exercise. Rather, the initial default parameters of each model were further adjusted using the scenario descriptions and resulting changes in model performance were examined. We also used the best-fit parameter sets to explore the long-term trends of outputs from the participating models and to investigate management impacts.

2.4. Performance evaluation

Model performance was evaluated using a statistical measure called Root Mean Squared Logarithmic Error (*RMSLE*). The *RMSLE* metric uses logarithmically transformed data and is suitable to evaluate data with a high degree of variation.

$$RMSLE = \sqrt{\frac{1}{n}\sum_{i=1}^{n}\left(ln(y_i) - ln\left(\widehat{y}_i\right)\right)^2} = \sqrt{\frac{1}{n}\sum_{i=1}^{n}\left(ln\left(y_i \Big/ \widehat{y}_i\right)\right)^2}$$

where y_i are the modelled data, $\widehat{y}_i$ the observed data and n the number of data points. The *RMSLE* quantifies the ratio between modelled and observed data, while balancing the weights of small and high values (Brown and Dvorzhak, 2019). In this study, for the observed data, the geometric mean of multiple measured data for each endpoint was used. A low *RMSLE* value (i.e. close to zero) indicates a good agreement between measurements and model predictions, and *vice versa*. For example, *RMSLE* equal to 0.69 means that the observed and predicted values differ on average by a factor of 2. *RMSLE* values are shown in two ways: those calculated with default parameter values ($RMSLE_{Default}$) and those with adjusted values ($RMSLE_{Calibrated}$). Percentage change, calculated as $(RMSLE_{Default} - RMSLE_{Calibrated})/RMSLE_{Default} \times 100$, quantifies the degree of improvement by calibration. Positive values indicate a percentage of improvement whereas negative values indicate a percentage reduction in model accuracy. Please note that default parameters in some models were based on data measured in Fukushima forests after the FDNPP accident.

3. Results

3.1. Model performance before and after calibration for the generic cedar/cypress scenario (Scenario A1)

Table 3 presents *RMSLE* values that evaluate model performances for the inventories in total soil and total tree, and the activity concentrations

Table 2
Overview of the participating models (structures, processes, parameters and numerical approaches).

		CMFW	FoRothCs	RIFE1	SOLVEG-II	TRIPS 2.0	TREE4
Structure	**Above-ground tree**	Yes (leaf, branches, bark, sap wood, heart wood)	Yes (leaf, branch, stem wood)	Yes (internal, external)	Yes (leaf, branch bark, branch wood, stem bark, stem wood)	Yes (leaf, branch, stem wood, bark)	Yes (leaf external/internal, branch bark, branch wood, stem wood, stem outer bark, stem inner bark)
	Tree root	No	No	No	Yes	Yes	Yes (coarse roots)
	Litter or fresh organic layer	Yes	Yes	Yes	Yes	Yes (not used in this study)	Yes
	Organic soil layer	Yes	Yes	Yes	No[b]	Yes	Yes
	Mineral soil layer (number of layers)	No	Yes (1)	Yes (1)	Yes (multi-layered)	Yes (2)	Yes (60)
Process	**Cs transfer type**	Constant transfer rate	Dynamic (transfer rates depend on biomass size)	Constant transfer rate	Time-dependent (except for the tree internal part)	Constant transfer rate	Constant/time-dependent transfer rate
	Main Cs transfer processes in soil	No	No	Yes (leaching from the layer, not used in this study)	Yes (adsorption/desorption to/from soil, fixation/mobilization to/from clay)	Yes (fixation/mobilization to/from clay)	Yes (organic matter decomposition, leaching from organic layer, convection, dispersion, reversible sorption, irreversible fixation)
	Tree biomass submodel	No	Yes	No	Yes	No	Yes
	Hydrological process (canopy; soil)	No	Yes (throughfall)	No	Yes (interception, throughfall; water flow in soil)	No	Yes (interception, throughfall, stemflow; evaporation, transpiration, drainage)
Parameter	**Method to estimate default parameter values**	Calibration	Literature survey, calibration	Calibration	Literature survey	Literature survey	Literature survey, calibration
	Total number of parameters (=A)	20	58[a]	11	41	28	~35–80 (variable: empirical semi-mechanistic)
	Number of the parameters adjusted for calibration (=B)	20	5	7	9	3	8–14
	Ratio B/A	1.00	0.09	0.64	0.22	0.11	~0.2
Numerical approach	**Calibration method**	Grid search	Approximate Bayesian Computation (ABC)	Optimization using the Bayesian approach	Manual fitting	Manual fitting	Monte Carlo techniques Minimization of cost functions (RMSLE)
	Deterministic or stochastic	Deterministic	Deterministic	Deterministic	Deterministic	Deterministic	Deterministic Stochastic
	Model output interval	Arbitrary time interval in linear or logarithmic scale	Monthly	Yearly	Half hourly	Daily	Daily (numerical time step: hourly)

[a] Including forest growth model and differs for deciduous forests.
[b] Considered as the surface layers of mineral soil with a high content of soil organic matter.

in tree functional compartments. The *RMSLE* values for default parameter settings show that the predictions by TRIPS 2.0 and FoRothCs were in good agreement with the measured inventories in total tree and soil without any parameter adjustment (0.37 and 0.35 for total tree and 0.10 and 0.11 for total soil, respectively). In general, higher *RMSLE* values were observed for the activity concentrations in foliage, branch, wood and bark compared to the inventories of total tree and soil. $RMSLE_{Default}$ averaged over the four tree compartments varied between 0.6 and 1.59 (between 0.48 and 0.68 for $RMSLE_{Calibrated}$), whereas those averaged over total soil and tree vary between 0.23 and 0.76 (between 0.21 and 0.42 for $RMSLE_{Calibrated}$). SOLVEG-II and CMFW demonstrated the greatest improvements by calibration in calculations of the activity concentrations in general (48% on average for both of the models), and especially for branches (81% and 78%, respectively) and bark (84% and 85%). For the activity inventories, calibration provided the greatest improvement in total tree calculations by SOLVEG-II (56%), and in total soil by TRIPS 2.0 (15%). Interestingly, some of the models provided even less accurate estimations with calibrated parameters than with the defaults (e.g. CMFW and FoRothCs for inventory), which suggests a complex interplay between uncertainties in the field data and those of different parameterization schemes. Although the dataset, based on measurements from 37 different forest sites, was judged to be representative of the specified scenario, there was still uncertainty within the measured endpoints. For some models, therefore, increasing the accuracy of calculated activity concentrations of tree components caused the accuracy of inventories of tree and soil to decrease. In addition, the FoRothC simulations didn't use the biomass provided in the scenario, but instead calculated the biomass using a sub-model.

After calibration, the average accuracy of the six model calculations was highest for the inventory of total soil (*RMSLE*: 0.15), whereas it was much lower in that of total tree (0.46) and in the activity concentrations in foliage, branches and wood (0.64, 0.45 and 0.73, respectively). The highest standard deviation over the six model calculations was shown for the activity concentrations in branches and wood (0.29). The TREE4 model demonstrated among the most accurate matches with both measured inventories and activity concentrations.

Best estimate calculations by calibrated models and measured data from 2011 to 2016 are shown in Fig. 1 for ^{137}Cs inventories in total tree and total soil, and in Fig. 2 for ^{137}Cs activity concentrations in foliage, branches, bark and wood. The differences in total tree fractions calculated by each model for 2011 were large, suggesting that the estimate of the interception of the initial fallout differs between models. However, as a group, the model calculations reproduced the general trends of the measured ^{137}Cs inventories in total tree and soil and enclosed most of

Table 3
Model performance (*RMSLE* values) before and after calibrations.

Model	Run	Inventory (dimensionless)[d]			Activity concentration (m^2 kg^{-1} d.m.)[d]				
		Total tree	Total soil	Average	Foliage	Branch	Bark	Wood	Average
CMFW	Default	0.45	0.09	0.27	0.69	0.80	1.83	0.57	0.97
	Calibrated	0.57	0.12	0.34	0.52	0.18	0.27	0.55	0.38
	Change (%)[a]	*−25*	*−31*	*−28*	*25*	*78*	*85*	*3*	*48*
FoRothCs	Default	0.35	0.11	0.23	0.74	0.77		0.65	0.72
	Calibrated	0.48	0.16	0.32	0.46	0.86		0.57	0.63
	Change (%)[a]	*−35*	*−36*	*−36*	*37*	*−13*		*12*	*12*
RIFE1[b]	Default	0.78	0.12	0.45				1.02	1.02
	Calibrated	0.45	0.18	0.31				0.60	0.60
	Change (%)[a]	*42*	*−47*	*−3*				*41*	*41*
SOLVEG−II	Default	1.35	0.18	0.76	0.93	1.77	2.32	1.34	1.59
	Calibrated	0.60	0.24	0.42	0.69	0.34	0.37	1.30	0.68
	Change (%)[a]	*56*	*−33*	*11*	*26*	*81*	*84*	*3*	*48*
TREE4	Calibrated[c]	0.32	0.11	0.21	0.71	0.24	0.25	0.73	0.48
TRIPS2.0	Default	0.37	0.10	0.23	0.88	0.59	0.33	0.59	0.60
	Calibrated	0.37	0.08	0.23	0.83	0.63	0.31	0.62	0.60
	Change (%)[a]	*0*	*15*	*8*	*6*	*−7*	*5*	*−6*	*−0.5*
All models	Average (Calibrated)	0.46	0.15		0.64	0.45	0.30	0.73	
	St. Dev. (Calibrated)	0.11	0.06		0.15	0.29	0.05	0.29	

[a] Calculated by: (Default − Calibrated)/Default × 100.
[b] Monthly values from the RIFE1 model (annual) were estimated by interpolating its annual output in order to allow comparisons with observations.
[c] TREE4 model provided only calibrated.
[d] The values were normalized with the total initial inventories (see the method section).

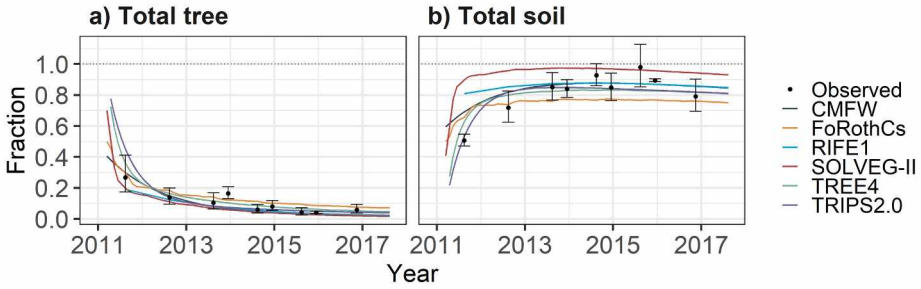

Fig. 1. Comparison of modelled and observed fractions of ^{137}Cs activity inventories in total tree (a) and soil (b) compartments to the total initial inventory. Log-transformed versions are provided in Supplementary Fig. S1. The observed data are indicated with points (GM) and error bars (GSD), respectively. The modelled predictions were generally provided on a monthly basis except for those of RIFE1 delivered on a yearly basis. TREE4 provided mean values averaged over all the possible predictions calculated using a stochastic approach.

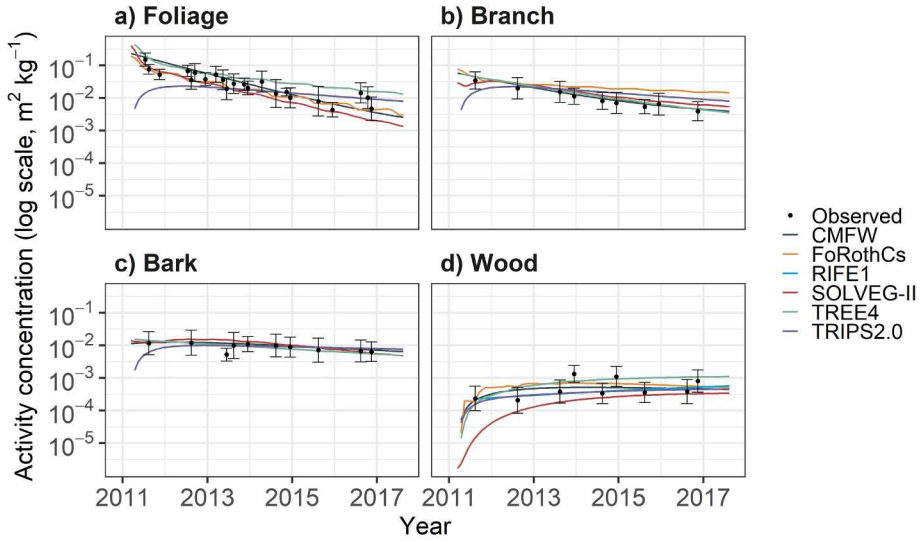

Fig. 2. Comparison of modelled and observed normalized ^{137}Cs activity concentrations for foliage (a), branches (b), bark (c) and wood (d). The observed data are indicated with points (GM) and error bars (GSD), respectively. The y axes are log-transformed; the linear scale version is shown in Supplementary Fig. S2. The modelled predictions were generally provided on a monthly basis except for those of RIFE1 delivered on a yearly basis. TREE4 provided mean values averaged over all the possible predictions calculated using a stochastic approach.

the measured points and ranges over a period of 6 years after the fallout. The spread of the set of calculations for total soil, averaged over 2011 to 2016, was about twice as high as that for total tree. The model calculation of TREE4 fall within the measured ranges at 7 time points, followed by TRIPS 2.0 at 6 time points. For the ^{137}Cs inventories in total soil, the modelled predictions of SOLVEG-II lie above the measured ranges at 7 of the 9 time points, whereas those of FoRothCs lie below the measured ranges at 5 time points. The other models demonstrated a close clustering from the second year of the calculations, lying in the middle of the over- and under-estimated outcomes.

Fig. 2 shows that model calculations as a whole were generally in agreement with the measured activity concentrations in each of the tree functional compartments. In particular, all model calculations for the bark compartment fall within the range of the measured values at 8 of the 9 time points. The apparent underestimation of foliage, branch and bark contamination by TRIPS 2.0 during the first to second years resulted from the model structure; the model separates the whole tree surface as an abiotic external compartment from the tree functional compartments (i.e. foliage, branches, wood and bark) (Thiry et al., 2020). The model calculations for the wood compartment showed that the activity concentration increased in the first 1–3 years, in particular in the first year, and then levelled off thereafter. The range of calculated ^{137}Cs activity concentrations for the wood compartment in 2017 was within one order of magnitude.

3.2. Long-term simulations

Figs. 3 and 4 show the best estimate calculations (i.e. after calibration) of the participating models over 50 years (between 2011 and 2061) for the same endpoints as shown in the previous figures. The simulations for the total tree inventory of ^{137}Cs generally demonstrated sharp decreases during the first 10 years, followed by moderate decreases to 0.1 and 1% of the initial deposition for the following years (Fig. 3 and Supplementary Fig. S3). The RIFE1 model exclusively showed a moderate increase after 10 years, resulting in the highest estimation at the end of the simulation period (Fig. S3). Simulated total soil ^{137}Cs inventories reached their peaks 3–4 years after the ^{137}Cs deposition, followed by constant decreases, which indicated a general agreement between the model simulations, although SOLVEG-II always lay slightly above the other models. The apparent overestimation by SOLVEG-II is caused by the model setting that includes a portion of global fallout.

The simulated ^{137}Cs activity concentrations for foliage and branches reached their peaks immediately after the initial deposition (except for TRIPS2.0 due to the particular model structure described above), followed by fast and then slow decreases (Fig. 4). TREE4 demonstrated the slowest reductions in foliage contamination. The simulations for bark contamination showed a close agreement for the first 10 years, then the model curves diverged with TRIPS2.0 showing the slowest decrease and SOLVEG-II the fastest. Fig. S4 clearly shows the divergence between individual model simulations for wood. RIFE1 calculated the highest peak ^{137}Cs activity concentration for wood, followed by TREE4. Compared to the other models, RIFE1 simulated this peak value with much delay, about 30 years after the ^{137}Cs deposition.

The annual changes in the ^{137}Cs fluxes from tree to soil and tree uptake, as calculated by each model, were examined (Fig. 5). In all the models, the outputs showed a clear decrease in tree to soil flux over the first 10 years, but the magnitudes of these fluxes differed between models. Decreasing tree to soil fluxes were mirrored by increasing tree root uptake fluxes in all models except SOLVEG-II and TREE4. The balance between tree to soil flux and root uptake 50 years after the fallout showed a variety of combinations; in CMFW, RIFE1 and TREE4, they almost balance while SOLVEG-II calculated that root uptake is smaller than tree to soil flux over the entire simulation period.

3.3. Management impact on ^{137}Cs dynamics (Scenarios B1 and B2)

The impacts of the two management scenarios were examined (Fig. 6). In the litter removal experiments (B1 scenario, Fig. 6b), the average activity concentration in wood was reduced 50 years after the accident; the maximum and minimum activity concentrations were lower than those in scenario A1 (the control scenario for generic cedar/cypress forests, Fig. 6a). The calculated ^{137}Cs activity concentrations in wood in 2061 ranged within two orders of magnitude. For some models, litter removal did not affect the activity concentrations (Fig. S5). The B2 management scenario (clear-cut and new planting) showed even more divergent trajectories between models (Fig. 6c). In particular, the ^{137}Cs activity concentration showed very large diversity after this management option was applied (years 2011–2020) (Fig. 6c and Fig. S5). Some models showed 10 times higher activity concentrations than those in scenario A1, while some models showed one–two orders of magnitude lower concentrations (Fig. S5). Fifty years after the accident, the range was comparable to that of the A1 scenario (Fig. 6c).

3.4. Applicability to deciduous broadleaf forests (Scenario C1)

The results of the preliminary application of the models to the ancillary konara oak scenario (scenario C1) are shown in Fig. 7, S6 and S7. All models successfully captured the increasing trend of the ^{137}Cs activity concentration in wood in the short term. The envelope of model predictions was smallest 4–5 years after the accident, although it enlarged thereafter. However, the envelope of predictions 50 years after the accident was still within one order of magnitude and smaller than that within the evergreen needleleaf scenario (A1; Fig. S7). The simulated trajectories were similar between models, but the timing of peaks and the rates of decrease in wood activity concentrations after the peak differed between models. The times of the peaks ranged from 5 to 15 years after the accident. In addition, the trajectories could be divided into two groups: relatively high activity concentrations in 2061 (CMFW, RIFE1 and TREE4) and lower activity concentrations (FoRothCs, SOLVEG-II and TRIPS2.0). A similar pattern was seen for the generic cedar/cypress scenario (A1).

4. Discussion

The main purpose of this exercise was to explore the performance and uncertainties (specifically, inter-model variability) of the six forest radionuclide models included in the study. The aims and scopes of the participating models were similar, although they had different components and numerical schemes which stem a) from differences in prior knowledge and applications, b) in processes which are considered of interest and most important and c) in the data used initially to calibrate each model. In terms of the number of parameters and compartments the simplest model was RIFE1: this model originally aimed to capture the overall dynamics of radionuclides within forests contaminated by the

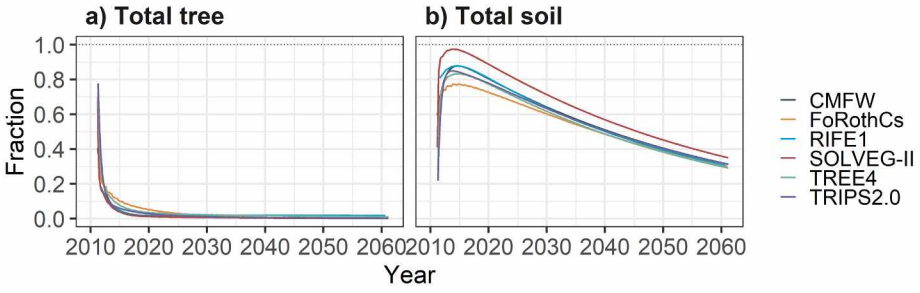

Fig. 3. Long-term simulations of ^{137}Cs activity inventories in total tree (a) and soil (b) compartments, for 50 years after the accident (expressed as a fraction of the total initial inventory). Log-transformed versions are provided in Supplementary Fig. S3.

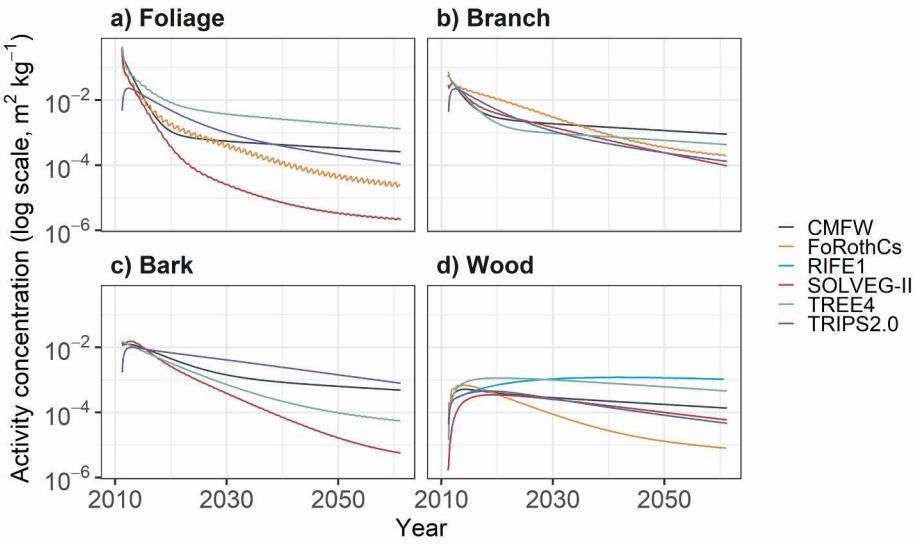

Fig. 4. Long-term simulations of normalized ^{137}Cs activity concentrations for foliage (a), branches (b), bark (c) and wood (d). The y axes are log-transformed; the linear scale version is in Supplementary Fig. S4.

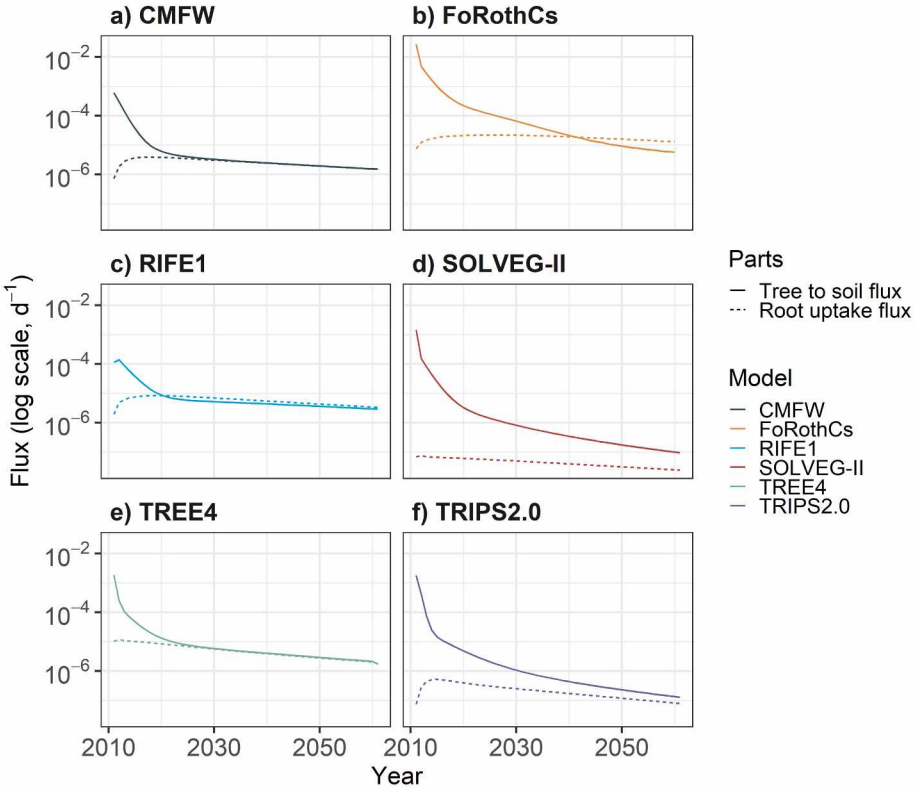

Fig. 5. Annual changes in the ^{137}Cs fluxes from tree to soil (solid lines) and tree uptake (dashed lines).

Chernobyl accident. It is not easy to tell which is the most complex model; TREE4, SOLVEG-II and the FoRothCs models are relatively complex models with small time steps and/or comprehensive hydrological, ecological and radiological processes in forests that require many parameters. However, even with more parameters and processes represented within a model, some parameters are not sensitive or easily quantified while others are very sensitive or less easily quantifiable. The comparison shown in Table 2 demonstrates the basic similarity in fundamental model concepts but it also shows the large diversity in detailed processes incorporated within the models.

Furthermore, the inter-comparison demonstrated that the calibration schemes differ between the models, which should more or less contribute to the observed differences in model performance. For example, for the CMFW, most parameters can be determined with statistical fitting using time series data, while SOLVEG-II adopts many parameters for processes from literature surveys. This diversity in modelling processes is reflected in model structure. In addition to the calibration scheme, the data used for model calibration affects the performance against the validation data. The parameter adjustments based on the scenario data in general improved the model performance. However, most participating models were developed after the Fukushima accident and had been parameterized with data taken in Fukushima

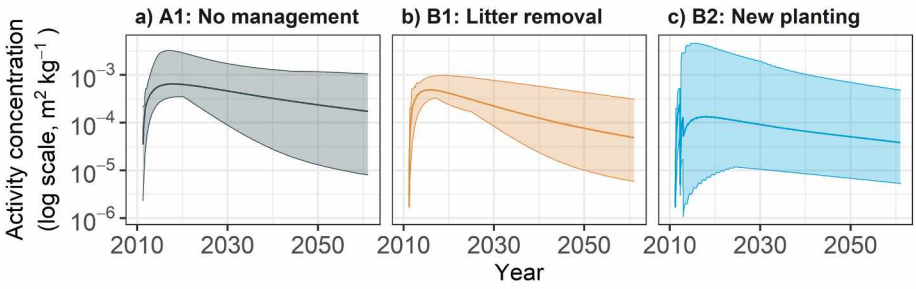

Fig. 6. Impact of the two management options (B1 and B2) on normalized ^{137}Cs activity concentrations for wood compared with no management (A1). The lines in the centre of the shaded ranges are geometric means, and the ranges show the minima and maxima of the model simulations. Individual model simulations are shown in Fig. S5.

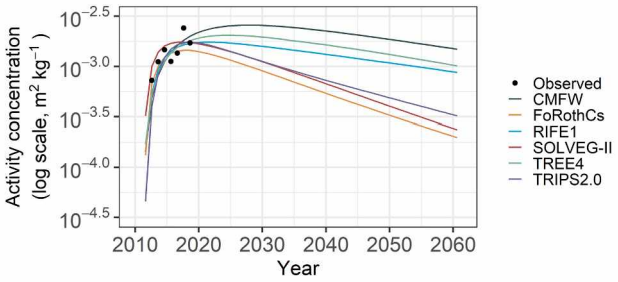

Fig. 7. Modelled and measured normalized ^{137}Cs activity concentration for wood in the oak scenario (C1). The data points are GM of the observed data.

forests. The RIFE1 and TRIPS2.0 models were used previously for post-Chernobyl studies, but they were also newly modified and parameterized with Fukushima data. Therefore, the performance improvements were limited for these models.

Despite the diversity of modeling principles, convergent trajectories (within one order of magnitude) were clearly seen in simulations of both tree/soil inventories and activity concentrations for each tree organ for the short-term period in the case of scenario A1. Some models showed the highest or lowest trajectories in the long-term, but the simulated ^{137}Cs activity concentrations in 2017 for wood were within one order of magnitude (Fig. 2). This range is comparable to results for simulations of ^{137}Cs in pine wood in the IAEA BIOMASS model inter-comparison after Chernobyl (Shaw et al., 2005). The same is applicable to simulations of ^{137}Cs in deciduous oak forest (scenario C1); although further tests are necessary, the models in general reproduced ^{137}Cs activities in konara oak trees quite well. Both the Chernobyl and Fukushima accidents happened in early spring, prior to the growth of new leaves for deciduous trees. If the fallout were to occur in a different season, the dynamics of radiocaesium in deciduous forests would be different. In addition, different contributions of wet or dry deposition at the time of fallout, and differences in how the models describe the interception of deposited radioactivity, would be important, particularly for the dynamics in the very early phase (e.g. days to months); some models describe the interception more mechanistically (e.g. SOLVEG-II and TREE4) while others did it through simply partitioning with constants or initial observed data (e.g. RIFE1 and TRIPS2.0). Analysis of these differences is outside the scope of this paper, but should be tested in the future.

When the models were compared in the long-term simulations for scenario A1, the variation between the models increased. The simulated activity concentrations for foliage, bark and wood increased with time and were within two orders of magnitude 50 years after the fallout (Fig. 4). It is very likely that the divergence observed between models in the long term is due to the fact that calibration against the 2011–2017 dataset enabled reliable estimation of model parameters involved in the short- and mid-term processes but less reliably for processes operating in the longer-term, such as reduction in ^{137}Cs bioavailability in the soil and the impact of this on root uptake. Another point to consider is that even a small error/difference in a kinetic rate induces an increasingly large error/difference in cumulative flux in the long term. In this model inter-comparison, we tested two popular forest management practices in Japan. The envelope of simulations 50 years after the fallout were, in general, within the same order as the no-management scenario (scenario A1), but the envelope of model outputs increased after approximately 5 years for clear cutting and new planting (scenario B2) (within three orders of magnitude; Fig. 6). Our inter-comparison was not designed to identify the mechanisms that caused the divergence of model predictions, but one probable cause of the higher predicted wood concentration for some models is the use of a constant root uptake coefficient in trees of all ages (e.g. RIFE1). More research should be done on root uptake by newly planted trees.

This inter-comparison was designed mainly to explore the envelope of output simulations by the ensemble of models and not to identify the detailed processes and parameters responsible for the variation of those simulations. However, the large envelopes of model simulations observed over 50 years in scenario A1could be attributable to the different representations of loss versus uptake dynamics of ^{137}Cs in trees (in particular, stem wood) between the participating models (Fig. 5). As summarized in Table 2, some models only consider ^{137}Cs loss by radioactive decay, while some account for other influential processes such as wood turnover (e.g, SOLVEG-II) and dilution effects due to tree (phytomass) growth that result in self-decontamination of wood over the decades following the fallout (i.e. after peak wood concentration is reached). In addition, there is large uncertainty in the simulations of ^{137}Cs activity concentrations in wood for newly planted trees. The contamination of newly planted trees should occur almost entirely via the root uptake of ^{137}Cs, indicating that the calculation of root uptake of ^{137}Cs differs significantly between the models; this can be partly seen in the large divergence (by two to three orders of magnitude) of fluxes calculated for the control case (shown in Fig. 5 and aggregated transfer factors shown in Fig. S8). The significant differences in calculated root uptake could be attributable to calculation of soil ^{137}Cs dynamics (Table 2); some models consider adsorption and fixation of ^{137}Cs in soil that limits root uptake whereas other models do not explicitly account for such reduction of bioavailability in soil ^{137}Cs due to fixation. These comparisons strongly indicate that long-term measurement for both pre-existing and newly-planted trees as well as soil ^{137}Cs and resulting root uptake can improve understanding and constrain models for ^{137}Cs cycling; this will improve the reliability of long-term predictions. In particular, as suggested by previous researchers (Goor and Avila, 2003; Goor and Thiry, 2004), the root uptake process is the most influential factor controlling the long-term contamination of wood because it is the key driver of the tree-soil ^{137}Cs cycle. However, direct quantification of root uptake *in situ* is challenging (Imamura et al., 2021). Even so, continued monitoring of tree contamination over the long-term will improve model parameterization of this process.

The convergence of model simulations in scenario A1 is probably due to the quite complete set of data characterizing ^{137}Cs partitioning in

Japanese cedar/hinoki cypress forests in the early phase after initial deposition in 2011. This period is generally characterized by a substantial and rapid redistribution of the initial ^{137}Cs deposits between trees and soil, partly controlling further ^{137}Cs recycling. Furthermore, the Japanese plantation forests are even-aged and quite homogeneous compared to natural forests, which enabled us to prepare generic data. The availability of adequate data in this scenario as well as in the literature seems to have facilitated the adjustment of transfer parameters for most models (e.g. Gonze et al., 2021; Hashimoto et al., 2020b). In post-Chernobyl studies, such complete data sets exist but were much more limited in geographic and temporal coverage (IAEA, 2002). This improvement of the dataset is a key development since the IAEA BIOMASS project, as well as the continued modification of the model structures in the participating models; some of the models were newly-developed after the Fukushima accident, and others are modified versions of models that participated in the IAEA BIOMASS project (see Table 1 and the model description in the Supplementary information).

In this inter-comparison, we focused on inter-model variability and did not include the individual uncertainties of each model. Inclusion of the uncertainty of each model output may enlarge the total uncertainty of the model predictions. Identifying the detailed processes and parameters responsible for both the inter-model variability and the uncertainty of each model is an important future task.

In the previous model inter-comparison exercise after the Chernobyl accident (Shaw et al., 2005), it was pointed out that data were available for only the first 10–12 years and that 'the forecasting capability of the models over future decades currently remains untested'. Unfortunately, we still do not have comprehensive long-term data for ^{137}Cs dynamics in forests, despite the 35 years which have elapsed since Chernobyl, due to a cessation of monitoring. The model inter-comparison reported in this paper was done with data taken in the early phase (rapidly changing phase), less than 10 years after deposition. To validate the forecasting capability of the models and to further refine the models, it is even more necessary to continue collecting long-term data, and to use this data to parameterize and validate forest radioecological models.

5. Conclusion

This study is the first inter-comparison of models designed to simulate radiocesium behaviour in forests using the data observed in the first decade after the Fukushima accident. The models successfully reproduced the observed ^{137}Cs activity concentrations and inventories in trees and soil over this period. The longer-term (50 years) simulations demonstrated a very strong agreement between models of predicted ^{137}Cs inventories in trees and soil; however, the inter-comparison also showed that the long-term simulation of activity concentrations of foliage, bark and wood differs considerably between the models. Large inter-model uncertainties were also observed for the scenario in which cutting and re-planting of trees was simulated. This inter-comparison has demonstrated the broad capabilities and the uncertainties of the forest radionuclide models currently being actively developed. However, it is essential to continue repetitive verification/validation processes using much longer-term data sets for various forest types to improve the forecasting capacity of the models.

Declaration of competing interest

The authors declare that they have no known competing financial interests or personal relationships that could have appeared to influence the work reported in this paper.

Acknowledgement

S.Hashimoto, M.K., N.K. and S.O. acknowledge JSPS KAKENHI Grant Number 16H04945, and S. Hashimoto, M.K. S.O. and N.I. acknowledge research grants from FFPRI (#201501, #201901). M.A.G., F.C., P.H. and Y.T. acknowledge the AMORAD project achieved thanks to the French State financial support managed by the Agence Nationale de la Recherche with funds allocated in the "Investissements d'Avenir" framework program under reference ANR11-RSNR-0002. This inter-comparison exercise is partly supported by the FFPRI and the AMORAD project.

Appendix A. Supplementary data

Supplementary data to this article can be found online at https://doi.org/10.1016/j.jenvrad.2021.106721.

References

Avila, R., Bergman, R., Scimone, M., Fesenko, S., Sancharova, N., Moberg, L., 2001. A comparison of three models of ^{137}Cs transfer in forest ecosystems. J. Environ. Radioact. 55, 315–327. https://doi.org/10.1016/S0265-931X(00)00199-5.

Brown, J., Dvorzhak, A., 2019. Guidance to Select Level of Complexity (European Joint Programme for the Integration of Radiation Protection Research H2020 – 662287 No. Ares(2019)4957171).

Calmon, P., Gonze, M.-A., Mourlon, Ch, 2015. Modeling the early-phase redistribution of radiocesium fallouts in an evergreen coniferous forest after Chernobyl and Fukushima accidents. Sci. Total Environ. 529, 30–39. https://doi.org/10.1016/j.scitotenv.2015.04.084.

Croom, J.M., Ragsdale, H.L., 1980. A model of radiocesium cycling in a sand hills—Turkey Oak (*Quercus laevis*) ecosystem. Ecol. Model. 11, 55–65. https://doi.org/10.1016/0304-3800(80)90071-X.

Diener, A., Hartmann, P., Urso, L., Vives i Batlle, J., Gonze, M.A., Calmon, P., Steiner, M., 2017. Approaches to modelling radioactive contaminations in forests – Overview and guidance. J. Environ. Radioact. 178–179, 203–211. https://doi.org/10.1016/j.jenvrad.2017.09.003.

Fesenko, S., Spiridonov, S., Avila, R., 1999. Modelling of ^{137}Cs behaviour in forest game food chains. In: Linkov, I., Schell, W.R. (Eds.), Contaminated Forests. Springer Netherlands, Dordrecht, pp. 239–247. https://doi.org/10.1007/978-94-011-4694-4_25.

Gonze, M.-A., Calmon, P., Hurtevent, P., Coppin, F., 2021. Meta-analysis of radiocesium contamination data in Japanese cedar and cypress forests over the period 2011–2017. Sci. Total Environ. 750, 142311. https://doi.org/10.1016/j.scitotenv.2020.142311.

Gonze, M.-A., Renaud, P., Korsakissok, I., Kato, H., Hinton, T.G., Mourlon, C., Simon-Cornu, M., 2014. Assessment of dry and wet atmospheric deposits of radioactive aerosols: application to Fukushima radiocaesium fallout. Environ. Sci. Technol. 48, 11268–11276. https://doi.org/10.1021/es502590s.

Goor, F., Avila, R., 2003. Quantitative comparison of models of ^{137}Cs cycling in forest ecosystems. Environ. Model. Software 18, 273–279. https://doi.org/10.1016/S1364-8152(02)00075-0.

Goor, F., Thiry, Y., 2004. Processes, dynamics and modelling of radiocaesium cycling in a chronosequence of Chernobyl-contaminated Scots pine (*Pinus sylvestris* L.) plantations. Sci. Total Environ. 325, 163–180. https://doi.org/10.1016/j.scitotenv.2003.10.037.

Hashimoto, S., Imamura, N., Kaneko, S., Komatsu, M., Matsuura, T., Nishina, K., Ohashi, S., 2020a. New predictions of ^{137}Cs dynamics in forests after the Fukushima nuclear accident. Sci. Rep. 10, 29. https://doi.org/10.1038/s41598-019-56800-5.

Hashimoto, S., Imamura, N., Kawanishi, A., Komatsu, M., Ohashi, S., Nishina, K., Kaneko, S., Shaw, G., Thiry, Y., 2020b. A dataset of ^{137}Cs activity concentration and inventory in forests contaminated by the Fukushima accident. Sci. Data 7, 431. https://doi.org/10.1038/s41597-020-00770-1.

Hashimoto, S., Matsuura, T., Nanko, K., Linkov, I., Shaw, G., Kaneko, S., 2013. Predicted spatio-temporal dynamics of radiocesium deposited onto forests following the Fukushima nuclear accident. Sci. Rep. 3, 2564. https://doi.org/10.1038/srep02564.

Hashimoto, S., Ugawa, S., Nanko, K., Shichi, K., 2012. The total amounts of radioactively contaminated materials in forests in Fukushima, Japan. Sci. Rep. 2, 416. https://doi.org/10.1038/srep00416.

Imamura, N., Komatsu, M., Ohashi, S., Hashimoto, S., Kajimoto, T., Kaneko, S., Takano, T., 2017. Temporal changes in the radiocesium distribution in forests over the five years after the Fukushima Daiichi Nuclear Power Plant accident. Sci. Rep. 7, 8179. https://doi.org/10.1038/s41598-017-08261-x.

Imamura, N., Watanabe, M., Manaka, T., 2021. Estimation of the rate of ^{137}Cs root uptake into stemwood of Japanese cedar using an isotopic approach. Sci. Total Environ. 755, 142478. https://doi.org/10.1016/j.scitotenv.2020.142478.

International Atomic Energy Agency, 2015. The Fukushima Daiichi Accident - Technical, 4/5. Radiological Consequences, Vienna.

International Atomic Energy Agency, 2006. Environmantal consequences of the Chernobyl accident and their remediation: twenty years of experience. https://www-pub.iaea.org/MTCD/publications/PDF/Pub1239_web.pdf.

International Atomic Energy Agency, 2002. Modelling the Migration and Accumulation of Radionuclides in Forest Ecosystems. Report of the Forest Working Group of the Biosphere Modelling and Assessment (BIOMASS) Programme (Theme 3).

Kurikami, H., Sakuma, K., Malins, A., Sasaki, Y., Niizato, T., 2019. Numerical study of transport pathways of ^{137}Cs from forests to freshwater fish living in mountain streams in Fukushima, Japan. J. Environ. Radioact. 208–209, 106005. https://doi.org/10.1016/j.jenvrad.2019.106005.

Nishina, K., Hashimoto, S., Imamura, N., Ohashi, S., Komatsu, M., Kaneko, S., Hayashi, S., 2018. Calibration of forest ^{137}Cs cycling model "FoRothCs" via approximate Bayesian computation based on 6-year observations from plantation forests in Fukushima. J. Environ. Radioact. 193–194, 82–90. https://doi.org/10.1016/j.jenvrad.2018.09.002.

Nishina, K., Hayashi, S., 2015. Modeling radionuclide Cs and C dynamics in an artificial forest ecosystem in Japan -FoRothCs ver1.0-. Front. Environ. Sci. 3, 61. https://doi.org/10.3389/fenvs.2015.00061.

Olson, J.S., 1965. Equations for cesium transfer in a liriodendron Forest. Health Phys. 11, 1385–1392.

Ota, M., Nagai, H., Koarashi, J., 2016. Modeling dynamics of ^{137}Cs in forest surface environments: application to a contaminated forest site near Fukushima and assessment of potential impacts of soil organic matter interactions. Sci. Total Environ. 551–552, 590–604. https://doi.org/10.1016/j.scitotenv.2016.02.068.

Riesen, T.K., 2002. Radiocaesium in forests — a review on most recent research. Environ. Rev. 10, 79–90.

Shaw, G., 2007. Radionuclides in forest ecosystems. In: Shaw, G. (Ed.), Radioactivity in the Environment. Elsevier, pp. 127–155. https://doi.org/10.1016/S1569-4860(06)10006-6.

Shaw, G., Avila, R., Fesenko, S., Dvornik, A., Zhuchenko, T., 2003. Chapter 11 Modelling the behaviour of radiocaesium in forest ecosystems. In: Scott, E.M. (Ed.), Radioactivity in the Environment, Modelling Radioactivity in the Environment. Elsevier, pp. 315–351. https://doi.org/10.1016/S1569-4860(03)80067-0.

Shaw, G., Venter, A., Avila, R., Bergman, R., Bulgakov, A., Calmon, P., Fesenko, S., Frissel, M., Goor, F., Konoplev, A., Linkov, I., Mamikhin, S., Moberg, L., Orlov, A., Rantavaara, A., Spiridonov, S., Thiry, Y., 2005. Radionuclide migration in forest ecosystems – results of a model validation study. J. Environ. Radioact. 84, 285–296. https://doi.org/10.1016/j.jenvrad.2003.09.006.

Shcheglov, A., Tsvetnova, O., Klyashtorin, A., 2014. Biogeochemical cycles of Chernobyl-born radionuclides in the contaminated forest ecosystems. Long-term dynamics of the migration processes. J. Geochem. Explor. 144, 260–266. https://doi.org/10.1016/j.gexplo.2014.05.026.

Thiry, Y., Albrecht, A., Tanaka, T., 2018. Development and assessment of a simple ecological model (TRIPS) for forests contaminated by radiocesium fallout. J. Environ. Radioact. 190–191, 149–159. https://doi.org/10.1016/j.jenvrad.2018.05.009.

Thiry, Y., Tanaka, T., Dvornik, A.A., Dvornik, A.M., 2020. TRIPS 2.0: toward more comprehensive modeling of radiocaesium cycling in forest. J. Environ. Radioact. 214–215, 106171. https://doi.org/10.1016/j.jenvrad.2020.106171.